Electronic Supplementary Material (ESI) for Polymer Chemistry.

Supplementary Material (ESI) for Polymer Chemistry

Soft and rigid core latex nanoparticles prepared by RAFT-mediated surfactant-free emulsion polymerization for cellulose modification – A comparative study

J. Engström,[a,b] F. L. Hatton[c], L. Wågberg,[c,b] F. D'Agosto,[d] M. Lansalot,[d] E. Malmström[a,b] and A. Carlmark[a,b*]

[a] *Fibre and Polymer Technology, KTH Royal Institute of Technology, 100 44, Stockholm, Sweden*
[b] *Wallenberg Wood Science Centre, KTH Royal Institute of Technology, 100 44, Stockholm, Sweden*
[c] *Université de Lyon, Univ Lyon 1, CPE Lyon, CNRS UMR 5265, C2P2 (Chemistry, Catalysis, Polymers & Processes), LCPP, 69616 Villeurbanne, France*
** Email: annac@kth.se*

Analysis of macroRAFT agent P(DMAEMA-co-MAA):

The degree of hydrolysis (DH) of DMAEMA monomer during aqueous synthesis of P(DMAEMA-*co*-MAA) macroRAFT agent[28] was determined by ^{1}H NMR analyses using the equation S1. $I_{3.26}$ and $I_{3.51}$ indicate integrals for the resonances at 3.26 ppm of the methylene adjacent to the amine of ethanolamine (formed by hydrolysis of DMAEMA) and at 3.51 ppm of the methylene adjacent to the tertiary amine in DMAEMA and PDMAEMA, respectively.

$$DH(\%) = \frac{I3.26}{I3.26 + I3.51} \times 100 \quad \text{Equation S1}$$

Table S1. Calculation of the degree of hydrolysis of DMAEMA during RAFT polymerization in water by integration of the signals for ethanolamine (3.26 ppm) and PDMAEMA un-hydrolyzed and any residual monomer (3.51 ppm), using 1,3,5-trioxane as internal reference (integral set to 1).

Time (min)	**0**	**5**	**10**	**20**	**30**	**40**	**50**	**60**	**90**	**120**	**full time**
I3.26	0.05	0.09	0.14	0.21	0.24	0.24	0.26	0.26	0.28	0.27	0.31
I3.51	7.28	7.61	7.23	7.29	7.71	6.89	7.22	7.05	6.84	6.74	7.49
Degree of hydrolysis (%)	0.68	1.17	1.90	2.80	3.02	3.37	3.48	3.56	3.93	3.85	3.97

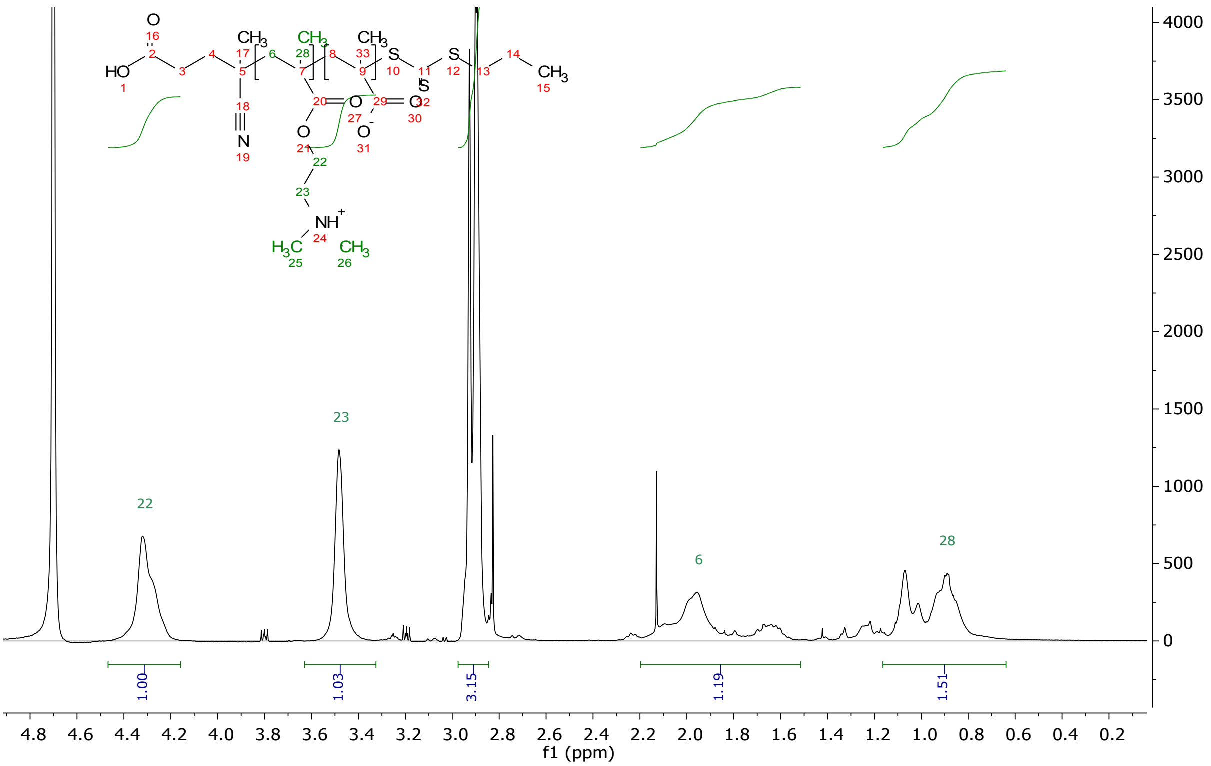

Figure S1. ^{1}H-NMR spectrum of macroRAFT agent P(DMAEMA-*co*-MAA) dissolved in D_2O. The chemical structure with its functional groups can be seen in the figure showing correlating peaks in NMR. There are some peaks originating from solvent after precipitation.

Analysis of PMMA and PnBMA latexes:

Table S2. Summarized data for all synthesized latex particle of PMMA and P*n*BMA, targeting a final dry content of 16.7 wt%. pH of reaction was kept at 6 and the ratio [macroRAFT]:[I] was kept at 8.25 for all reactions.

Sample	$[\text{macroRAFT}]_0$ (mM in H_2O)	$[M]_0$ (mM in H_2O)[a]	Added mL H_2O	Added mL AIBA (aq) (at conc. 3.4 gL^{-1})	N_P (10^{14} $mL^{-1}{}_{Latex}$)[b]
$PMMA_{176}$ latex	9.2	1.61	19.211	1.870	37.0
$PMMA_{705}$ latex	2.7	1.89	39.632	1.052	4.30
$PMMA_{1410}$ latex	1.4	1.94	43.359	0.584	1.19
P*n*BMA_{176} latex	6.9	1.21	26.363	1.870	25.7
P*n*BMA_{705} latex	1.9	1.35	37.163	0.701	6.03
P*n*BMA_{1410} latex	1.0	1.38	36.758	0.351	2.47

[a] The concentration of monomer, targeting degree of polymerization of 176, 705 and 1410. [b] The number of particles per mL latex is calculated from equation 1 and taking into account the D_H from DLS measurements.

Table S3. DLS data from analysis of latex particles in MilliQ water, sodium phosphate buffer and 1 mM KCl solution.

Sample	D_H (nm)[a]	PdI (DLS)[a]	Zeta potential (mV)[a]	D_H (nm)[b]	PdI (DLS)[b]	D_H (nm)[c]	PdI (DLS)[c]	Zeta potential (mV)[c]
$PMMA_{176}$ latex	42	0.08	58.0	36	0.07	44	0.14	41.2
$PMMA_{705}$ latex	89	0.05	60.6	74	0.02	80	0.02	40.0
$PMMA_{1410}$ latex	134	0.03	57.8	120	0.03	120	0.03	39.6
P*n*BMA$_{176}$ latex	50	0.12	55.1	42	0.09	47	0.12	43.3
P*n*BMA$_{705}$ latex	83	0.07	56.8	79	0.05	77	0.09	38.1
P*n*BMA$_{1410}$ latex	104	0.05	51.5	96	0.05	100	0.07	40.2

[a] Latex in MilliQ water at 3 g L^{-1} in terms of polymer dry weight. [b] Latex in 5 mM sodium phosphate buffer at 0.1 g L^{-1} in terms of polymer dry weight. [c] Latex in 1 mM KCl solution at 0.1 g L^{-1} in terms of polymer dry weight.

Adsorption of PnBMA latexes onto cellulose model surfaces in QCM-D:

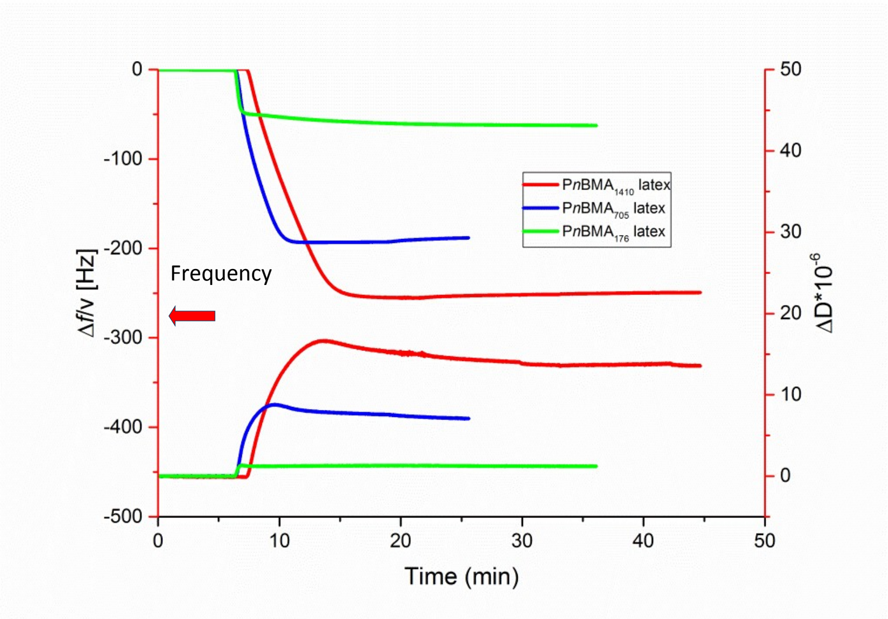

Figure S2. QCM-D adsorption of P*n*BMA latex particles at 0.1 g L^{-1} concentration at 0.15 mL min^{-1} flow in MilliQ water on cellulose model surfaces. The adsorption is finalized with rinsing step using MilliQ water.

Calculations for adsorbed latexes onto cellulose model surfaces in QCM-D:

Calculations of the adsorbed charges in the form of latex particles based on QCM-D adsorption on cellulose model surface considering P*n*BMA$_{176}$ latex (D$_H$ = 42 nm) and P*n*BMA$_{1410}$ latex (D$_H$ = 96 nm), the following equation S2 can be used, assuming the dry content of the adsorbed film to be 50 %. Using charge density from PET of P*n*BMA$_{176}$ latex (0.43 µeq g^{-1}) and P*n*BMA$_{1410}$ latex (0.087 µeq g^{-1}):

$$Charge\ density\left[\frac{\mu eq}{g}\right] * mass\ adsorbed\left[\frac{mg}{m^2}\right] = \frac{charge}{area}\left[\frac{\mu eq}{m^2}\right]$$

Equation S2

For the calculation of surface coverage as spherical close packing the following equation S3 can be applied, still assuming 50 % solids content in the layer on the crystal:

$$\pi * \frac{DH_2}{2} * \frac{nr(particles)}{gram} * \frac{mass}{m^2}(dry\ weight) = \frac{area\ particles}{area\ crystal}\left[\frac{m^2 particles}{m^2 substrate}\right]$$

Equation S3

Where the number of particles per gram, abbreviated nr(particles)/gram, is 2.58 x 10^{16} g^{-1} for P*n*BMA$_{176}$ latex and 2.15 x 10^{15} g^{-1} for P*n*BMA$_{1410}$ latex from density 1 and geometry of a sphere, and mass m^{-2} is 5.25 and 22.2 for P*n*BMA$_{176}$ latex (D$_H$ = 42 nm) and P*n*BMA$_{1410}$ latex (D$_H$ = 96 nm), respectively.

Contact angle measurement and AFM imaging of QCM crystal with PEI and CNF layer made in QCM-D:

Figure S3. Contact angle image of the QCM-D crystal formed *in situ* with layers of PEI and CNF before subsequent treatment with 5 mM sodium phosphate buffer at pH 6.8 before annealing.

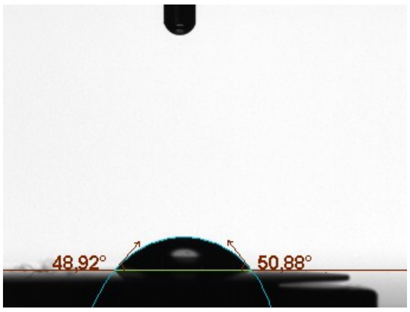

Figure S4. Contact angle image of the QCM-D crystal formed *in situ* with layers of PEI and CNF before subsequent treatment with 5 mM sodium phosphate buffer at pH 6.8 after annealing at 160 °C for 1 h.

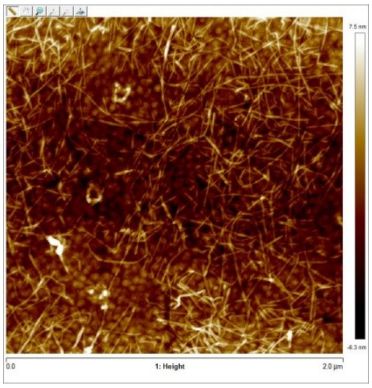

Figure S5. AFM image of the QCM-D crystal formed *in situ* with layers of PEI and CNF before subsequent treatment with 5 mM sodium phosphate buffer at pH 6.8.

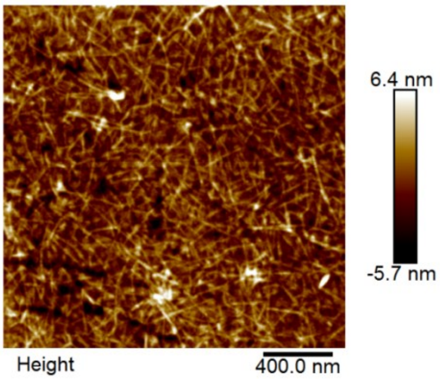

Figure S6. AFM image of the QCM-D crystal formed *in situ* with layers of PEI and CNF before subsequent treatment with 5 mM sodium phosphate buffer at pH 6.8 after annealing at 160 °C for 1 h.

Table S4. Contact angle measurement on filter papers after latex adsorption.

Sample	**CA before annealing (°)**	**CA after annealing (°)**
No latex reference	- [a)]	- [a)]
$PMMA_{176}$ latex	- [a)]	124
$PMMA_{705}$ latex	- [a)]	118
$PMMA_{1410}$ latex	- [a)]	122
P*n*BMA_{176} latex	125	131
P*n*BMA_{705} latex	128	131
P*n*BMA_{1410} latex	118	132

[a)] Absorbs water droplet

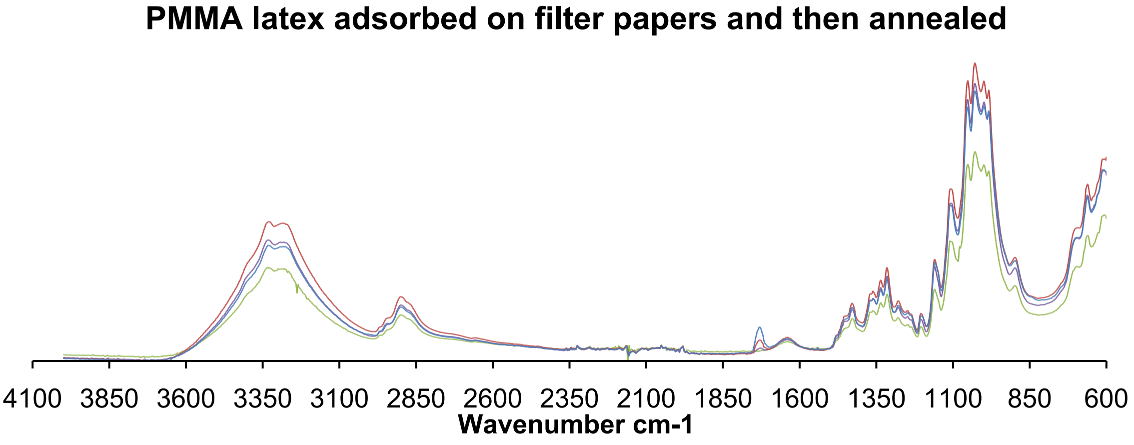

Figure S7. FTIR spectra of PMMA-based latexes adsorbed onto filter paper and annealed at 160 °C: $PMMA_{176}$ latex (blue line), $PMMA_{705}$ latex (red line), $PMMA_{1410}$ latex (purple line) and a reference filter paper (green line).

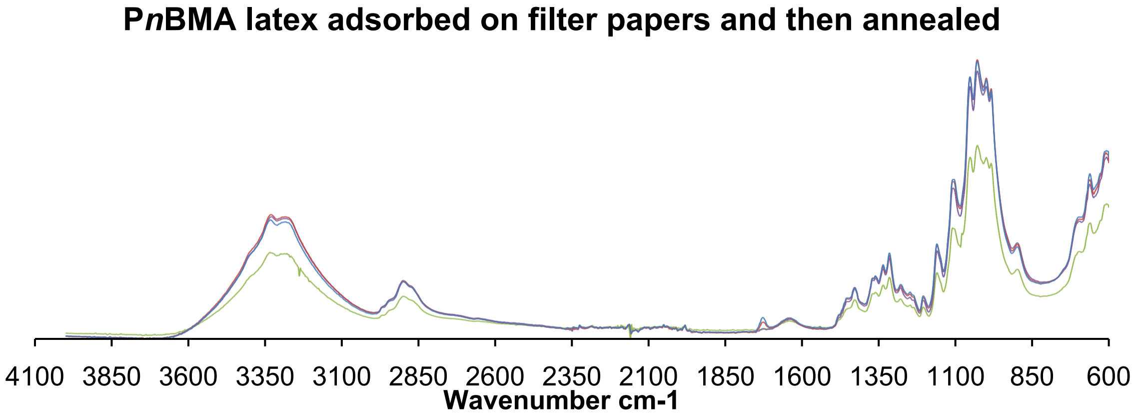

Figure S8. FTIR spectra of P*n*BMA-based latexes adsorbed onto filter paper and annealed at 160 °C: P*n*BMA$_{176}$ latex (blue line), P*n*BMA$_{705}$ latex (red line), P*n*BMA$_{1410}$ latex (purple line) and a reference filter paper (green line).

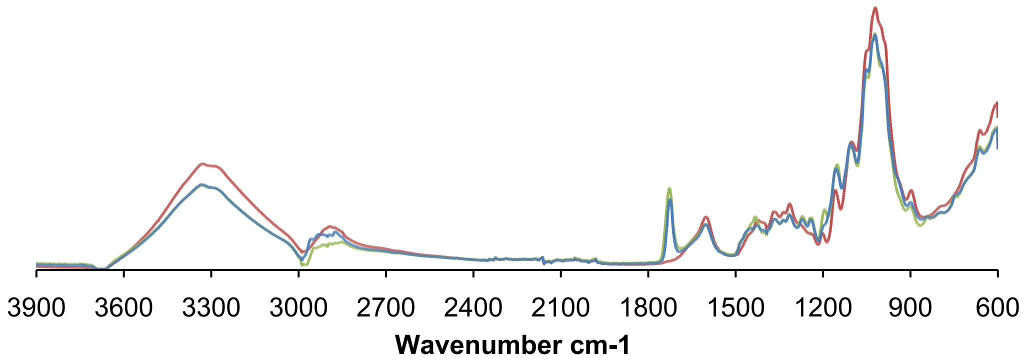

Figure S9. FTIR spectra of CNF composite films: CNF reference (red), CNF P*n*BMA$_{1410}$ latex (blue) and CNF PMMA$_{1410}$ latex (green).